C. K. Babulal

P. S. Kannan

Department of Electrical and Electronics Engineering Thiagarajar College of Engineering, Madurai–625 015, INDIA.

ck_babulal@yahoo.co.in.
psk_kannan@yahoo.co.in.

J. Electrical Systems 2-3 (2006): 146-161

Regular paper

A Novel Approach for ATC Computation in Deregulated Environment

This paper presents a novel method for determination of Available Transfer Capability (ATC) based on fuzzy logic. Adaptive Neuro-Fuzzy Inference System (ANFIS) is used to determine the step length of Homotophy continuation power flow method by considering the values of load bus voltage and change in load bus voltage. The approach is compared with the already available method. The proposed method determines ATC for various transactions by considering thermal limit, voltage limit and static voltage stability limit and tested in WSCC 9 bus system, New England 39 bus system and Indian 181 bus system.

Keywords: Available Transfer Capability, Voltage Stability, Fuzzy logic.

1. INTRODUCTION

Around the world, the vertically integrated structures in electric power supply are changing to competitive and deregulated framework. In the new electricity markets, transmission grids are going to operate closer to their thermal limits. Hence, it is important to know how much power can be transferred from a point to point or from generators to loads in a power system at this moment and in the future from the viewpoint of system operation and planning. Additionally in deregulated circumstances of the power system, it has already become possible for the third party such as independent power producers and customers to have an access to the transmission network for wheeling. Under the above condition, it becomes more and more important to calculate ATC as precisely and efficiently as possible considering thermal line flow limit, bus voltage limit and voltage stability limit.

Available transfer capability is a measure of the transfer capability remaining in the physical transmission network for further commercial activity over and above already committed uses. Mathematically, ATC is defined as the Total Transfer Capability (TTC) less the Transmission Reliability Margin (TRM), less the sum of existing transmission commitments (ETC), which includes retail customer service and the capacity benefit margin,

$$\mathrm{ATC} = \mathrm{TTC} - \mathrm{TRM} - \mathrm{ETC}$$

In recent years, a number of methods have been reported in literature for ATC determination. So far, there are three major approaches suggested for the calculation of ATC.

(i) Sensitivity analysis

(ii) Optimal power flow (OPF)

(iii) Continuation power flow (CPF)

Sensitivity analysis is the earliest solution proposed for the ATC approximation value calculation [1, 2]. Based on linear incremental power flow the sensitivity factors are simple to define and easy to calculate [3, 4]. The major disadvantage of the Linearized approach is it does not take into account the non-linear effects of reactive power and voltage [5].

Moreover, the methods based on power transfer/outage distribution factors [6, 7] can cater to only the scenarios that are too close to the base case from which the factors are derived.

OPF and security-constrained OPF are widely used for pool type transaction or power corridors between the power system in determining ATC or TTC [8-10]. However, in the case of open access power system, transaction may occur in practice from any point to any point. Bilateral transaction from source bus to sink bus is not at all an optimization problem.

CPF is first introduced for determining the maximum loadability; however, it is adaptable for other applications including ATC computation without changing its principle. The advantage of CPF is that it will not encounter numerical difficulties of ill conditioned power flow equations, thus CPF yields solutions even at voltage collapse points [10, 11]. Earlier use of CPF in determining ATC [12] reveals that the complexity and computational time increases when the contingency analyses are introduced for all possible cases. Consequently, as such it is not suitable for on-line applications in its present form.

However, the drawback of large number of iterations involved in CPF method could be eliminated by the use of fuzzy logic. The advantage of fuzzy logic is it tackles the dimensionality of a problem in a computationally efficient manner and can capture uncertainties inherently present in the system. The other approach reported in [13] using artificial neural network requires a large input vector for bilateral transaction, so it has oversimplified the determination of ATC by limiting it to a special case of power transfer to a single area from all of the remaining areas. Therefore, this method is also unable to track down the bus-to-bus transactions, which is the true spirit of deregulation.

Recently, in [14] fuzzy logic based ATC determination is proposed, which takes sink bus load, neighboring bus injection, and loading index as input signal for fuzzy system. It is reported in the paper that, the difference in the ATC values calculated by load flow method and fuzzy method is in the order of 100 to 250MW. Moreover, different fuzzy systems are adopted for calculating ATC, when the topology of the system changes [14].

In this paper, a new method for evaluating ATC based on adaptive neuro-fuzzy inference system is proposed. ANFIS is used to determine the step length of Homotophy continuation power flow method (HCM) by considering the values of load bus voltage and change in load bus voltage. In [15] the effectiveness of fuzzy logic controller in determining critical loading point is explored with various case studies. In [16], ANFIS is used to determining the static voltage stability limit. The same principle used [16] is adopted in this paper to determine ATC for various transactions by considering line thermal limit, voltage limit and static voltage stability limit. One ANFIS system is used for each test case presented and it is able to handle the topological changes in the power system.

The rest of the paper is organized as follows: Section 2 discusses the Homotophy continuation method. Section 3 presents ANFIS in HCM. The algorithm of the proposed method is presented in section 4. Case studies on the WSCC 9 bus and New England 39 bus and Indian 181 bus system are demonstrated in the section 5 and conclusion in section 6.

2. HOMOTOPHY CONTINUATION METHOD

The HCM is documented in [17]. In HCM, the critical loading condition and nose curves are obtained by solving the Homotophy function (1):

$$H(x,t) = Y(x) - Y_s(t) \tag{1}$$

$$Y_s(t) = Y_{s0} + t.Y_d \tag{2}$$

where Y_{s0} - specified value of base load in p.u.

Y_d - loading/generating pattern

t - Homotophy scalar parameter

$Y_s(t)$ - loading pattern linear above the base load

x - voltage vector in p.u.

The solution of $H(x,t) = 0$, provides a load flow solution for specified value of $Y_s(t)$. This method is summarized below.

Step 1. Using the conventional load flow program, the load flow problem is solved to obtain the voltage vector at a base load condition.

Step 2. Y_d is set according to the operating guidance and k in (3) is chosen according to the size of the Jacobian matrix J.

Step 3. Δt and Δx are calculated using (3) and (4):

$$\Delta t = \sqrt{k/(1 + \sum(J^{-1}.Yd)^2)} \tag{3}$$

$$\Delta x = \Delta t \,.\, J^{-1}.\, Yd \tag{4}$$

where Δt – step length and Δx – change in bus voltage

Step 4. The auto scaling function in (5):

$$\Delta t^2 + \Sigma \Delta x^2 = K \tag{5}$$

is used to calculate an appropriate step size Δt.

Step 5. A solution $(x_0 + \Delta x, t_0 + \Delta t)$ that adjoins a known solution (x_0, t_0) is predicted by satisfying the linear relationship between Δx and Δt in (6):

$$J.\Delta x - Y_d.\Delta t = 0 \tag{6}$$

Step 6. The intermediate solution is stored in x and t are updated. The procedure is repeated until the desired accuracy is reached. The terminal point $Y_s(t)$ is the critical loading point.

3. ANFIS

The design objective of the fuzzy controller is to learn and achieve good performance in the presence of disturbances and uncertainties. The design of membership functions is done by the ANFIS batch learning technique, which amounts to tune a FIS with back propagation algorithm based on a collection of input – output data pairs.

3.1 ANFIS Architecture

Generally, ANFIS is a multilayer feed forward network in which each node performs a particular function (node function) on incoming signals. For simplicity, we consider two

inputs 'x' and 'y' and one output 'z'. Suppose that the rule base contains two fuzzy if-then rules of Takagi and Sugeno type [18].

Rule 1: IF x is A1 and y is B1 THEN $f_1 = P_1x + Q_1y + R_1$

Rule 2: IF x is A2 and y is B2 THEN $f_2 = P_2x + Q_2y + R_2$ (7)

The ANFIS architecture shown in figure 1 is a five layer feed forward network as follows.

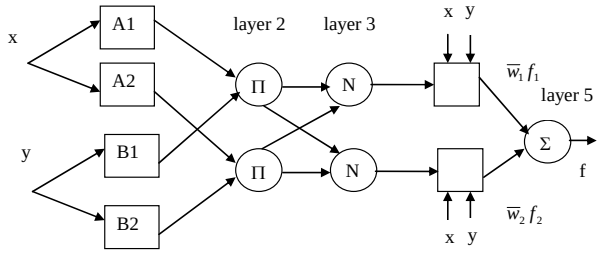

Figure 1. The ANFIS Architecture.

Layer 1: Every node in this layer is a square node with a node function (the member ship value of the premise part)

$$O_i^1 = \mu_{Ai}(x) \quad (8)$$

Where, x is the input to the node i, and Ai is the linguistic label associated with this node function.

Layer 2: Every node in this layer is a circle node labeled Π which multiplies the incoming signals. Each node output represents the firing strength of a rule.

$$O_i^2 = \mu_{Ai}(x)\, \mu_{Bi}(y) \text{ where } i = 1{:}2 \quad (9)$$

Layer 3: Every node in this layer is a circle node labeled N (normalization). The i^{th} node calculates the ratio of the i^{th} rule's firing strength to the sum of all firing strengths.

$$O_i^3 = \overline{W_i} = \frac{W_i}{W_1 + W_2} \text{ , where } i = 1{:}\ 2 \quad (10)$$

Layer 4: Every node in this layer is a square node with a node function

$$O_i^4 = \overline{W}_i f_i = \overline{W}_i (P_i x + Q_i y + R_i) \text{ , where } i = 1{:}2 \quad (11)$$

Layer 5: The single node in this layer is a circle node labeled Σ that computes the overall output as the summation of all incoming signals

O_i^5 = System output, where i = 1:2 (12)

Equation (12) represents the overall output of the ANFIS, which is functionally equivalent to the fuzzy system in (7).

3.2 ANFIS learning algorithm

In this subsection the hybrid learning algorithm is explained briefly. The hybrid learning algorithm is a combination of both the back propagation and the least square algorithms. The back propagation is used to identify the nonlinear parameters (premise parameters) and the least square is used for the linear parameters in the consequent parts.

From the ANFIS structure given above, it has been observed that when the values of the premise parameters are fixed, the overall output can be expressed as a linear combination of the consequent parameters. That is the output in layer 5 "Eq. (6)" can be rewritten as

$$f = \frac{W_1}{W_1 + W_2} f_1 + \frac{W_2}{W_1 + W_2} f_2$$

$$f = \overline{W_1}\, f_1 + \overline{W_2}\, f_2$$

$$f = \overline{W_1}(P_1 x + Q_1 y + R_1) + \overline{W_2}(P_2 x + Q_2 y + R_2)$$

$$f = (\overline{W}_1 x)P_1 + (\overline{W}_1 y)Q_1 + (\overline{W}_1)R_1 + (\overline{W}_2 x)P_2 + (\overline{W}_2 y)Q_2 + (\overline{W}_2)R_2 \qquad (13)$$

This is linear in the consequent parameters P_1, Q_1, R_1, P_2, Q_2 and R_2.

From this observation, the whole system parameter set can be represented as $S = [S_1 S_2]$ where S_1 is the set of nonlinear parameters and S_2 is the set of linear parameters. The hybrid learning algorithm is a combination of both back propagation and the least square algorithms. Each epoch of the hybrid learning algorithm consists of two passes, namely forward pass and backward pass. In the forward pass of the hybrid learning algorithm, functional signals go forward up to layer 4 and the consequent parameters are identified by the least squares estimate.

3.3 ANFIS Step Length Controller

The functional block diagram of the ANFIS step length controller is shown in figure 2.

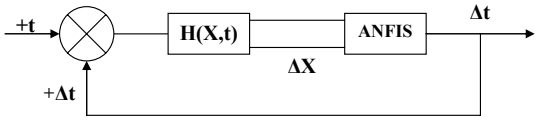

Figure 2. Functional Block Diagram of ANFIS Step Length Controller

Where x and Δx are load bus voltage and change in load bus voltage in p.u. Δt is the incremental loading parameter. The ANFIS step length control has two inputs, the bus voltage and change in bus voltage, and one output step length. Figure 3 shows the architecture of the ANFIS step length controller.

The design steps are as follows:

1. The computational efficiency of any continuation power flow method is depends on the choice of effective step length control [19]. Ideally the step length should be selected according to the shape of the nose curve to be traced, and it is unknown beforehand. Thus, making the task of designing the effective step length control difficult. From the nose curve or PV curve of the system, it is clear that, when the system is operating near the base case, the decrease in bus voltage due to an increase in load is less. In contrast, decrease in voltage will be large when the system is

operating near the critical loading. This leads to an idea of choosing larger step length at lightly loaded conditions and smaller step length at stressed condition.

2. The performance of ANFIS controller is depends on the size of the training data set. Thus the training data for the step length controller should cover the wide range of all possibilities of bus voltages and change in bus voltages.

3. The training data for the ANFIS step length controller is selected from the Homotophy continuation method, as given section 2.

4. This training data yields the membership functions for the input variables, which are shown in figure 4.

5. ANFIS is trained using 100 epochs and an initial step size of 10-4 which was the best step found that gives acceptable error convergence.

6. The number of membership functions, their range and the amount of overlapping are changed in order to fit the training data output.

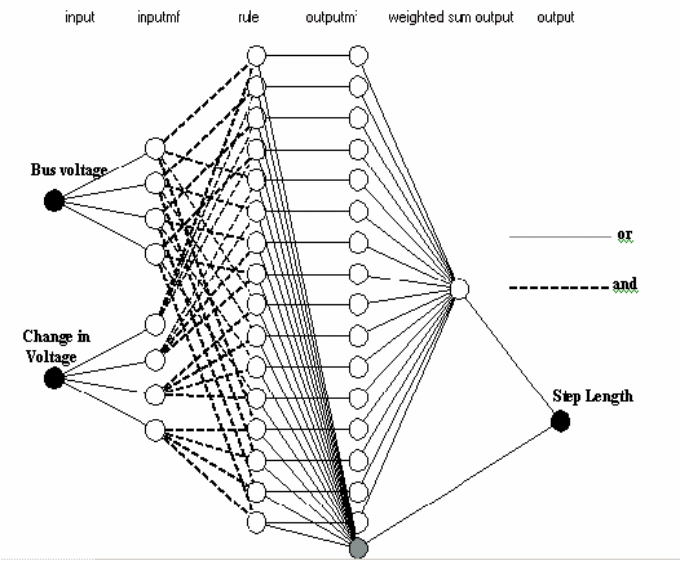

Figure 3. Architecture of ANFIS Step Length Controller

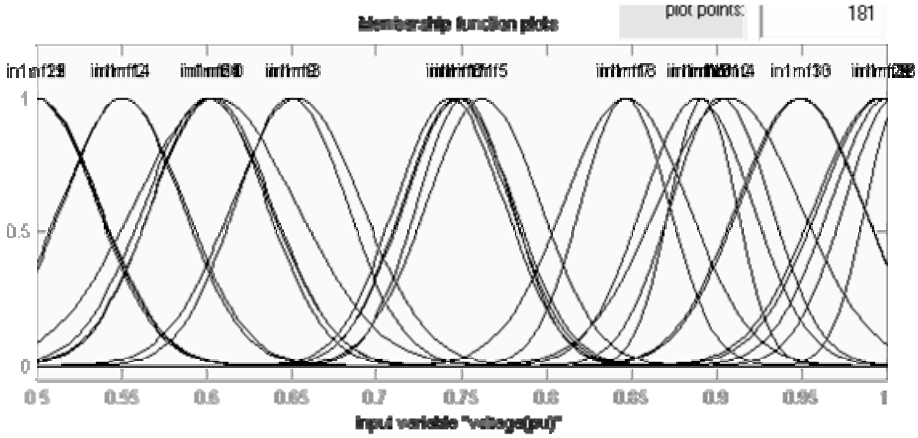

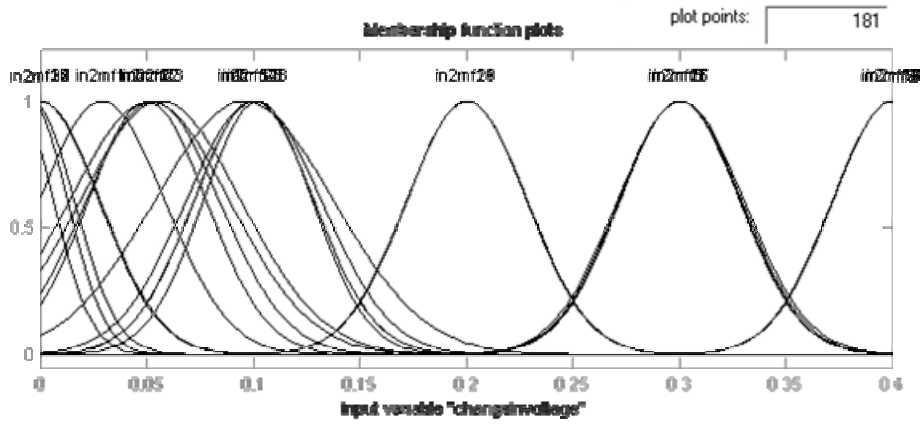

Figure 4. Membership Function of Input Variables

4. PROPOSED APPROACH ALGORITHM

The following steps in general explain the procedure involved in determining ATC.

1. The load flow problem is solved to obtain the base case results.
2. Typical transaction from seller bus to buyer bus is selected
3. For bilateral/pool type transaction, the generation in the seller bus/area is increased and the load at the buyer bus/area is increased by the same amount.
4. The PV curves at the load buses are traced using FLC in HCM as explained in the section 2 and 3.
5. Suppose, if any one of the transmission line hit the thermal limit, then ATC is determined using (14) otherwise, execution goes to step 3.

$$ATC_{mn,TL} = P_{ij} - P_{ij}^{0} \text{ in MW} \quad (14)$$

where, $ATC_{mn,TL}$ is the value of ATC when a transaction is taking place between seller bus/area m and buyer bus/area n considering thermal limit violation. P_{ij} is power flow in the line connected between the bus i and j. P_{ij}^{0} is power flow at base case in the line connected between the bus i and j.

6. Suppose, if any one of the load bus violates the voltage limit (i.e., ±10% from nominal value of 1.0 p.u.) then, the ATC is determined using (15) otherwise, execution goes to step 3.

$$ATC_{mn,VL} = P_{ij} - P_{ij}^{0} \text{ in MW} \quad (15)$$

where, $ATC_{mn,VL}$ is the value of ATC when a transaction is taking place between seller bus/area m and buyer bus/area n considering voltage limit violation.

7. Suppose, if any one of the load bus experiences the maximum loadability limit then, the ATC is determined using (16).

$$ATC_{mn,VSL} = P_{ij} - P_{ij}^{0} \text{ in MW} \quad (16)$$

where, $ATC_{mn,VSL}$ is the value of ATC when a transaction is taking place between seller bus/area m and buyer bus/area n considering voltage stability limit.

5. CASE STUDY

The WSCC 9 bus system, New England 39 bus system and practical Indian 181 bus system have been considered for simulation studies. In a deregulated environment power transfer can occur in practice from any point of generation to any point of load. Some typical transactions between generator bus and load buses are considered for illustration purpose. In all the considered transactions, both real and reactive loads are increased with constant power factor. To verify the robustness of the ANFIS several other possible transactions and contingency analysis are carried out, but not reported in the paper. All the studies are conducted on P IV, 1500MHz computer using the program developed in MATLAB language.

5.1 WSCC 9 bus System [20]

The one line diagram, base case loading and the thermal limit of the WSCC 9 bus system are given in figure 5, table 1 and table 2 (given in appendix) respectively.

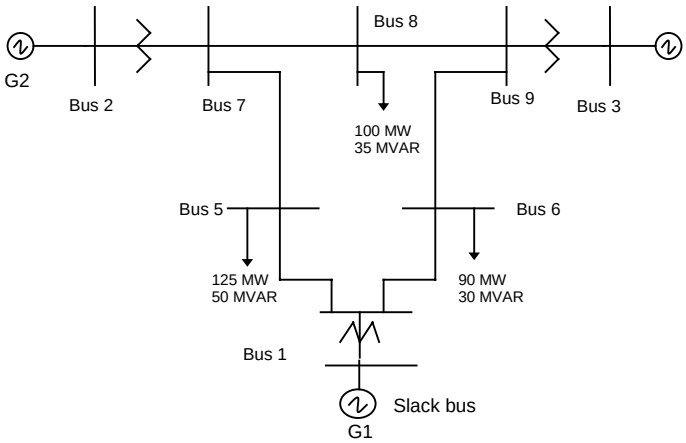

Figure 5. Single line diagram of WSCC 9 bus system

The following transactions have been considered.

(i) Transaction ‘T1’ generator 1 alone supplies the increase in load at bus 5

(ii) Transaction ‘T2’ generator 2 alone supplies the increase in load at bus 5

(iii) Transaction ‘T3’ generator 3 alone supplies the increase in load at bus 5

(iv) Transaction ‘T4’ generator 1&2 alone supplies the increase in load at bus 5

(v) Transaction ‘T5’ generator 2&3 alone supplies the increase in load at bus 5

(vi) Transaction ‘T6’ generator 1&3 alone supplies the increase in load at bus 5

(vii) Transaction ‘T7’ generator 1, 2 & 3 supplies the increase in load at bus 5

5.1.A Comparison between ANFIS and PSAT

The result obtained by the ANFIS is accurate as that of other methods, in this paper the effectiveness of the ANFIS in HCM is compared with the PSAT [21]. PSAT is a MATLAB based software routine, it uses predictor and corrector approach for the voltage stability

analysis. Though several test systems are compared with PSAT, only results of the WSCC 9 bus system for some of the transaction is presented in the table 3. Table 3 presents the value of real and reactive load at the nose point of the PV curve determined by PSAT and ANFIS. It is clear from the table 3 that, ANFIS could able to determine the CLP in less number of steps than the PSAT.

Table 3: Comparison between ANFIS and PSAT

Load at Bus #	Transaction	PSAT			ANFIS		
		P (MW)	Q (MVAr)	Number of Steps and time (sec)	P (MW)	Q (MVAr)	Number of Steps and time (sec)
5	T1	308.38	233.31	42(3.1)	331.16	214.93	11(1.2)
5	T4	290.06	215.69	38(3)	303.53	192.82	9(1.02)
5	T6	299.06	223.54	41(3.1)	319.19	205.35	10(1.2)
5	T7	265.57	190.57	33(2.85)	276.176	170.94	7(1)
6	T1	278.03	218.03	42(3.2)	323.39	185.59	14(1.3)
6	T4	271.25	211.25	41(3.2)	287.35	161.56	14(1.35)
6	T6	268.37	208.37	41(3.2)	287.75	161.83	12(1.25)
6	T7	240.79	180.79	35(2.9)	226.24	120.83	10(1.2)
8	T1	346.97	281.97	54(3.5)	393.01	240.1	17(2.1)
8	T4	332.11	267.11	52(3.4)	350.56	210.39	15(1.3)
8	T6	344.35	279.35	55(3.5)	379.1	230.38	15(2.0)
8	T7	326.07	261.07	21(2)	319.94	188.96	13(1.3)

5.1.B Calculation of ATC

The ATC values obtained while considering the different limits viz., thermal, voltage and voltage stability are depicted in table 4. Except for the transactions T3 and T5 thermal limit is found to be the limiting factor for ATC. The load increase at bus 6 and bus 8 were also studied but not reported.

Table 4: ATC of WSCC 9 bus system

Transaction	$ATC_{mn,TL}$	$ATC_{mn,VL}$	$ATC_{mn,VSL}$
T1	65.36	156.77	229.23
T2	84.07	89.99	130.8
T3	No violation	84.22	104.48
T4	117.05	133.78	166.37
T5	No violation	79.34	92.47
T6	73.24	154.89	234.36
T7	144.6	127.13	157.53

5.2 New England 39 bus system

The FLC developed for WSCC 9 bus system as such do not work for other systems. Therefore, the ANFIS controller is used, which determine the membership function using the set of input – output data. The one line diagram with the splitting of Area 1, 2 and 3 are given in figure 6. The system data is taken from the reference [22]. Line thermal limits of the New England 39 bus system are not available. Hence, reasonable assumption is made and given in appendix table 5 .

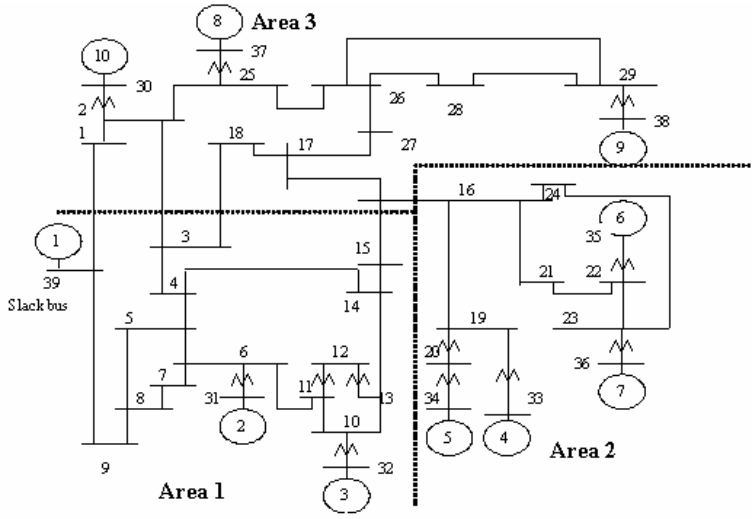

Figure 6. Single line diagram of New England 39 bus system

The following transactions are considered for the system.

(i) Transaction 'T1' generators in area 1 alone supplies the increase in load at area 2.

(ii) Transaction 'T2' generators in area 1 alone supplies the increase in load at area 3.

(iii) Transaction 'T3' generators in area 2 alone supplies the increase in load at area 3.

The ATC values obtained while considering the different limits viz., thermal, voltage and voltage stability are depicted in table 6. The other possible transactions are from area 2 to area 1, from area 3 to area 1 and area 3 to area 2 were also studied but not reported.

Table 6: ATC of New England 39 bus system

Transaction	$ATC_{mn,TL}$	$ATC_{mn,VL}$	$ATC_{mn,VSL}$
T1	80.128	2192.34	2276.77
T2	173.572	1812.29	1821.05
T3	298.127	1760.34	1959.77

5.3 Indian 181 bus system

Finally, the proposed technique has been tested in a practical Tamilnadu power system in India. The single line diagram of the reduced system is shown in figure 7 with the splitting of Area 1, 2 and 3. The system bus data, line data and generator data of the Indian 181 bus system were provided by the Power System Training Institute, Bangalore and Tamilnadu Electricity Board (TNEB).

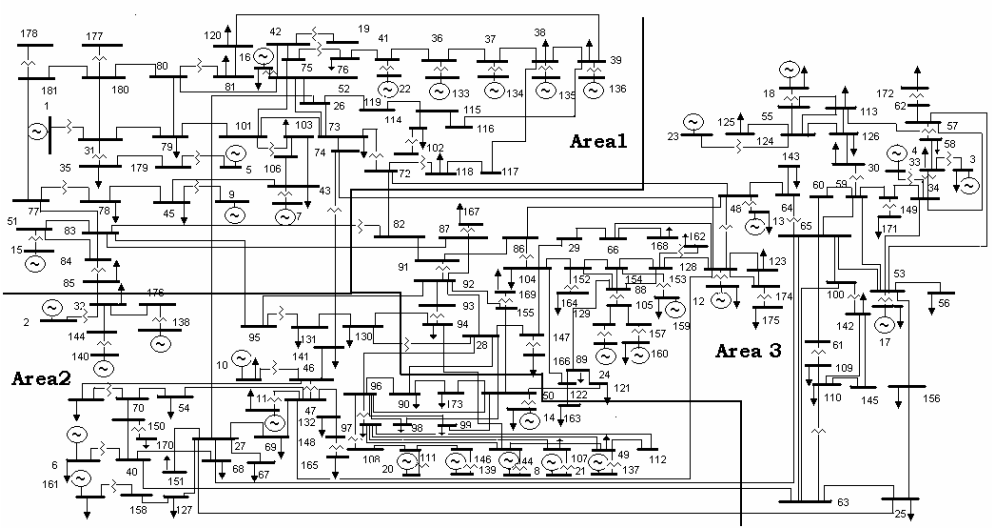

Figure 7. Single line diagram of Indian 181 bus system

Though the electrical supply scheme in India is completely different from the study undergone in this paper; the objective of the paper is to explore various possibilities that could arise in the deregulated environment in future.

The base case loading of the system is 6017.86 MW. Some of the important stations experiencing low voltages in view of limit violations are given in appendix table 7. Some stations like 109, 110, 121, 130, 131, 142, 145 and 167 experience low voltage (near to 0.9 p.u.) even in the base case loading.

In this system both pool type and bus to bus transactions are considered. The same pool type transactions considered in the New England 39 bus system is used in this system. Table 8 presents the ATC values obtained for pool type transaction.

Table 8: ATC of Indian 181 bus system

Transaction	$ATC_{mn,TL}$	$ATC_{mn,VL}$	$ATC_{mn,VSL}$
T1	383.45	1008.2	1466.41
T2	519.46	1230.05	1714.84
T3	388.86	1220.33	1856.25

In transaction T1, voltage limits are violated in the buses 89, 91, 94, 97, 108, 112, 114, 163, 166 along with the buses violated in the base case. The voltage collapse has occurred due to very low voltage of 0.6782 p.u. at bus number 130.

In transaction T2, voltage limits are violated in the buses 89, 114, 122, 163, 166, 168, 172 along with the buses violated in the base case. The voltage collapse has occurred due to very low voltage of 0.6124 p.u. at bus number 167.

In transaction T3, voltage limits are violated in the buses 89, 91, 114, 122, 163, 164, 166, 168, 172 along with the buses violated in the base case. The voltage collapse has occurred due to very low voltage of 0.5076 p.u. at bus number 167. ATC values obtained for the bus to bus transactions are given in Table 9.

Table 9: ATC of Indian 181 bus system bus to bus transaction

Transaction From – to	$ATC_{mn,TL}$	$ATC_{mn,VL}$	$ATC_{mn,VSL}$
16-175	153.32	239.34	274.29
14-25	108.06	478.22	762.63
16-127	89.33	225.47	499.71
13-45	208.01	227.33	441.72
13-127	166.44	229.39	511.96
14-45	153.46	203.44	333.53

The amount of additional power available for further transaction while considering thermal, voltage and voltage stability are determined for all possible combinations and some of the results are reported.

4. CONCLUSION

A new approach in determining ATC is presented. The proposed methodology is effectively utilizes the inherent information in the system based on fuzzy logic, which is not available in traditional methods. The effectiveness of the method is demonstrated with WSCC 9 bus system, New England system and a practical Indian 181 bus system. The FLC calculate ATC with less number of iteration and time as that of traditional methods. However, the ANFIS approach suffer from training data. There are other types of stability can limit the ATC values is not addressed in this paper.

Acknowledgement

The authors wish to thank the Management, Principal and Staff of Thiagarajar College of Engineering, Madurai, for providing necessary facilities to carry out this work. The authors thank the authorities of Power System Training Institute, Bangalore and Tamilnadu Electricity Board for providing the Indian 181 bus system. The help of Dr. Federico Milano in using PSAT is greatly acknowledged.

REFERENCES

[1] Available Transfer Capability Definitions and Determination, Technical Report: NERC, USA, 1996

[2] M. IIic, F. Galiana, L. Fink, A. Bose, P. Mallet and H. Othman, Transmission Capacity in Power Networks, Electrical Power and Energy Systems, Vol.20, no2, pp.99-110, 1998

[3] R. D. Christie, B. F. Wollenberg and I. Wangensteen, Transmission Management in the Deregulated Environment, Proceedings of the IEEE, Vol.88, no 2, pp.170-195, 2000

[4] A. Kumar, S. C. Srivastava and S. N. Singh, Available Transfer Capability (ATC) Determination in a Competitive Electricity Market Using AC Distribution Factors, Electric Power Components and Systems, Vol.32, no 9, pp. 927-939, 2004

[5] Y. H. Song, X. F. Wang (Eds.), Operation of Market-oriented Power Systems. Springer, 2003

[6] G. C. Ejebe and J. G. Waight, Manuel Santos-Nieto, and William F. Tinney, Fast Calculation of Linear Available Capability, IEEE Trans. Power systems, Vol.15, no 3, pp.955-960, 2000

[7] S. K. Chaudhary, S. C. Srivastava and A. Kumar, Available Transfer Capability Determination using Bifurcation Criteria and its Enhancement through SVC Placement, in: Proc. of the 12th NPSC, IIT Kharagpur, pp. 721-726, 2002

[8] G. M. Huang and P. Yan, TCSC and SVC as Redispatch Tools for Congestion Management and TTC Improvement, in: IEEE Power Engineering Society Winter Meeting, 2002

[9] Y. Ou and C. Singh, Improvement of Total Transfer Capability Using TCSC and SVC, in: IEEE Power Engineering Society Summer Meeting, 2001

[10] S. H. Goh, Z. Y. Dong and T. K. Saha, Security-Constrained Power System Transfer Capability Assessment, in: AUPEC 2003, Christchurch, New Zealand, September 2003

[11] C. A. Canizares, editor, Voltage Stability Assessment: Concepts, Practices and Tools, Tech. rep., IEEE/PES Power System Stability Subcommittee, August 2002

[12] G. C. Ejebe, J. Tong, J. G. Waight, J. G. Frame, X. Wang and W. Tinney, Available Transfer Capability Calculations, IEEE Trans. Power Systems, Vol.13, no 4, pp.1521–1527, 1998

[13] X. Luo, A. D. Patton, and C. Singh, Real Power Transfer Capability Calculations using Multi-layer Feed-forward Neural Networks, IEEE Trans. Power Systems, Vol.15, no 2, pp. 903–908, 2000

[14] A. B. Khairuddin, S. S. Ahmed, M. W.r Mustafa, A. A. Mohd Zin, and H. Ahmad, A Novel Method for ATC Computations in a Large-Scale Power System, IEEE Trans. Power Systems, Vol.19, no 2, pp.1150–1158, 2004

[15] C. K. Babulal, P. S. Kannan, J. Mary Anita and B. Venkatesh, Determination of Voltage Stability Limit Using Fuzzy Logic, Accepted for publication in the International Journal of Power and Energy Systems, 2006.

[16] C. K. Babulal, P. S. Kannan, J. Mary Anita, A Novel Approach to Determine Static Voltage Stability Limit and Its Improvement Using TCSC and SVC, Journal of Energy and Environment, Vol. 5, pp. 125 – 143, May 2006

[17] K. Iba, H. Suzuki, M. Egawa and T. Watanabe, A Method for Finding a Pair of Multiple Load Flow Solutions in Bulk Power Systems, IEEE Trans. on Power Systems, Vol.6, no 2, pp.584-593, 1991

[18] J-S Jang, ANFIS: Adaptive network based fuzzy inference system, IEEE Trans. on Systems, Man and Cybernatics Vol.23, no 3, pp. 665 – 685, 1993

[19] H. D. Chiang, A. J. Flueck, K. S. Shah and N. Balu, CPFLOW: A Practical Tool for Tracing Power System Steady State Stationary Behavior due to Load and Generation Variation, IEEE Trans. on Power Systems, Vol.10, no 2, pp. 623-633, 1995

[20] P. M. Anderson and A. A. Fouad, Power System Control and Stability: Galgotia publications, 1981

[21] F. Milano, Power System Analysis Toolbox, PSAT: MATLAB Software Available at http://www.power.uwaterloo.ca/~fmilano

[22] M. A. Pai, Energy Function Analysis for Power System Stability: Kluwer academic publications, July 1989

Appendix

Table 1: WSCC 9 bus system: Bus data at base case loading

Bus Number	V_0 p.u.	P_{L0} MW	Q_{L0} MVar	P_{G0} MW	V_{max} p.u.	V_{min} p.u.
1	1.04	0	0	71.61	1.1	0.9
2	1.025	0	0	163	1.1	0.9
3	1.025	0	0	85	1.1	0.9
4	1	0	0	0	1.1	0.9
5	1	125	50	0	1.1	0.9
6	1	90	30	0	1.1	0.9
7	1	0	0	0	1.1	0.9
8	1	100	35	0	1.1	0.9
9	1	0	0	0	1.1	0.9

Table 2: WSCC 9 bus system: Thermal limit

Line Number	Line between buses	Thermal limit MW
1	2-7	250
2	7-8	200
3	8-9	200
4	9-3	200
5	9-6	200
6	6-4	200
7	4-1	200
8	4-5	100
9	5-7	200

Table 5: Thermal limit of New England 39 bus system

No.	Line between buses	Thermal limit MVA
1	1-2	250
2	1-39	250
3	2-3	750
4	2-25	500
5	2-30	500
6	3-4	250
7	3-18	100
8	4-5	250
9	4-14	500
10	5-6	1000
11	5-8	500
12	6-7	750
13	6-11	500
14	6-31	1000
15	7-8	500
16	8-9	250
17	9-39	250
18	10-11	750
19	10-13	500
20	10-32	1000
21	11-12	100
22	12-13	100
23	13-14	500
24	14-15	100
25	15-16	500
26	16-17	500
27	16-19	1000
28	16-21	500
29	16-24	250
30	17-18	500
31	17-27	250
32	19-33	1000
33	19-20	250
34	20-34	1000
35	21-22	1000
36	22-23	250
37	22-35	1000
38	23-24	750
39	23-36	1000
40	25-26	250
41	25-37	1000
42	26-27	500
43	26-28	250
44	26-29	500
45	28-29	500
46	29-38	1000

Table 7: Some of the stations in Indian 181 bus system experiencing low voltage.

Bus #	Station Code
89	KARKUDI2
91	MADURAI4
94	THENI – 1
97	KAYATHR1
108	KAYATHR6
109	KADAPRI1
110	SPKOIL-1
112	SNKOIL-I
114	TRCHCOD1
121	PRMKUDY2
122	PUDKOTA2
130	MADURAI21
131	SEMBATI1
142	TARMANI1
145	VELCHRY1
163	PDUKOTI1
164	THNJVR1
166	MDRNRTH1
167	PUGALUR1
168	PERMBLR1
172	MYLAPOR1